CHEMELECTROCHEM

Supporting Information

Enhancing the Electrochemical and Electronic Performance of CVD-Grown Graphene by Minimizing Trace Metal Impurities**

Rodrigo M. Iost,[a, b] Frank N. Crespilho,[b] Laura Zuccaro,[a] Hak Ki Yu,[c] Alec M. Wodtke,[c] Klaus Kern,[a, d] and Kannan Balasubramanian*[a]

celc_201402325_sm_miscellaneous_information.pdf

SUPPORTING INFORMATION

I. Experimental Details

Materials. Sulfuric acid (H_2SO_4)(97-99%), H_2O_2 (30%) and HCl (36%) were obtained from Roth. All other chemicals were from Sigma. Graphene on copper was either purchased from Graphene Supermarket Inc. or grown on a peeled-off epitaxial Cu (111) foil. [18]

Transfer and patterning of graphene . All glasses utilized for the preparation of reagents were previously cleaned with concentrated HCl and washed with ultrapure water (Milli-Q system, 18 MΩ cm^{-1}). For Si/SiO_2 substrates, piranha solution H_2SO_4:H_2O_2 (3:1) was used for cleaning for at least 30 minutes and washed with ultrapure water and isopropanol before the transfer of graphene. CVD-graphene was cut into square pieces (typically 3cm x 3cm) and a solution of poly(styrene) (PS) (5 mg mL^{-1} in toluene) was spotted over the copper foil (PS/graphene/copper/graphene) and dried at 75ºC for 10 minutes. After the deposition of PS, the underlying copper was removed by etching in a solution of hydrochloric acid with added hydrogen peroxide (1.4M HCl + 0.5M H_2O_2) for at least 15 minutes. Then, graphene was transferred to Si/SiO_2 chips with prepatterned Ti/Pt electrode lines and baked in the oven at 95ºC for 10 minutes before removal of PS using toluene. The chips were then annealed at 585ºC for 40 seconds to improve the contact between graphene and the electrodes / substrate. The Hall bar structures were patterned using photolithography. For some devices, optionally 10 nm of copper was first evaporated on graphene to be used as a sacrificial protective layer in order that the photoresist does not come in direct contact with the graphene surface. The Hall bars are patterned using a positive process using the resist S1805 (Microposit). After exposure and development the unprotected regions are removed using a mild oxygen plasma etch. After this, the resist and the remaining copper are removed in *N*-ethylpyrrolidone and HCl/H_2O_2 respectively. We ensure that both for electrical as well as electrochemical measurements, all electrodes except graphene are passivated using an insulating layer. For this purpose we either deposit SiO_2 by thermal evaporation or use a resin at the locations of the electrode lines. This ensures that graphene is exclusively in contact with the solution.

Raman and AFM Images. Raman spectra of graphene samples on Si/SiO_2 chips were measured using an NT-MDT NTEGRA system, with a laser excitation of 632.8 nm at a power of 2.7 mW. This system was equipped with a 520 mm monochromator and a 600 l/mm grating. The acquisition time was 5s. AFM images were obtained using a Digital Instruments

Veeco Dimension III in tapping mode. The acquired AFM images were processed using Gwyddion software.

Electrochemical and Electrical Transport Measurements. Electrochemical experiments were performed in a 15 mL cell with graphene as working electrode, 0.5 mm Pt wire as auxiliary/counter electrode and Ag/AgCl as reference electrode using an Ivium Compactstat potentiostat. We have performed the e-etching always under ambient conditions in the presence of oxygen. In deaerated solutions the peaks were very weak consistent with the slow corrosion rate of copper in such solutions. [30] Hall bar measurements were made using a home-built magnetoresistance measurement setup in liquid, with a PDMS channel holding the buffer solution on top of the Hall bar samples. The gate voltage is applied using an Ag/AgCl reference. 4-probe resistance (R_{xx}) and the magnetoresistance (R_{xy}) are measured using a permanent magnet (0.3 T, calibrated using a Gaussmeter) for three different magnetic fields (0, +*B*, -*B*) at every gate voltage. The carrier concentration (n) and the Hall mobility (μ) as a function of applied gate voltage are extracted subsequently from these measurements.

Deposition of copper. The deposition of copper on graphene or flexible carbon fibers (FCF) was carried out by high energy electron beam (voltage of 2-10 kV) in a low vacuum chamber (typically 10^{-3} to 10^{-5} Torr) at T > 250ºC. A perpendicular electron beam evaporates copper, while the chips are placed in a rotating calotte. The rotation of the calotte is responsible for the homogeneous distribution of the metal film. The vacuum of the chamber creates a "cloud" that condenses over the substrate growing the metal film over the sample. The thickness of the film was controlled physically using an electrical oscillator at a deposition rate of 2 Å s^{-1} or less resulting in copper film of 100 Å thickness.

II. Simplified Pourbaix diagram of Cu : H_2O system

In order to obtain the simplified Pourbaix diagram we follow a scheme [30] by considering three solid species : copper, copper (I) oxide and copper (II) oxide; and two aqueous species : Cu^+ and Cu^{2+}. The Gibb's free energy of formation [31] is given by the following table:

Species	*Gibb's free energy of formation (kJ/mol)*
Cu	0
Cu_2O	-147.9
CuO	-128.29
Cu^+	48.87
Cu^{2+}	65.04

H_2O	-237.14

Based on these values we can arrive at the following equilibrium reactions along with their corresponding potential-pH behavior:

#1. $Cu_2O + 2e^- + 2H^+ \rightleftharpoons 2Cu + H_2O$ $\quad E = E^0 + \frac{0.0591}{2} log a_{H^+}^2$ $\quad E^0$=0.249V

#2. $Cu^{2+} + 2e^- \rightleftharpoons Cu$ $\quad E = E^0 + \frac{0.0591}{2} log a_{Cu^{2+}}$ $\quad E^0$=0.115V

#3. $2Cu^{2+} + 2e^- + H_2O \rightleftharpoons Cu_2O + 2H^+$

$$E = E^0 + \frac{0.0591}{2} log \left(\frac{a_{Cu^{2+}}}{a_{H^+}}\right)^2 \qquad E^0 = -0.019 \text{ V}$$

#4. $2CuO + 2e^- + 2H^+ \rightleftharpoons Cu_2O + H_2O$

$$E = E^0 + \frac{0.0591}{2} log (a_{H^+})^2 \qquad E^0 = 0.447 \text{ V}$$

#5. $Cu^{2+} + H_2O \rightleftharpoons CuO + 2H^+$

$$\Delta G = -2.303\, RT\, log \frac{a_{H^+}^2}{a_{Cu^{2+}}} \qquad \Delta G = 45 \text{ kJ/mol}$$

We neglect equilibria involving Cu^+(aq) since it is not stable and not relevant here (since there is no dissolved copper in solution). The E^0 values and the equations presented above are for Ag/AgCl as reference electrode. We then sketch lines for the above equations for varying activities of the ions ($a_{Cu}{}^{2+}$) and using pH = $-\, log(a_{H+})$. In figure 1, an ion activity of 10^{-4} has been assumed in order to obtain an approximate agreement with the measured oxidation peaks. More elaborate diagrams for the Cu:H_2O system and the Cu:Cl^-:H_2O system can be found elsewhere. [32,33]

III. Evaluation of copper removal on flexible carbon fibers

We gather further support that the observed phenomena are indeed related to copper / copper oxide by evaluating the electrochemical behavior of flexible carbon fiber electrodes (FCF) that are obtained by electrospinning of organic precursors. [34] In contrast to other carbon nanostructures, FCF is "free" of metal/metal oxide impurities since there are no metal

precursors involved during their preparation. This is confirmed by a typical CV of an FCF electrode shown in figure S4(a) (black curve), where no peaks are observed in the relevant potential region. Now we deliberately deposit copper (10 nm) on the FCF electrode and measure the CV, which is shown as the red curve in figure S4(a). A broad oxidation peak is observed in the same potential range as for the graphene samples due to chloride formation. Subsequently, we apply the same e-etching procedure on this electrode (see figure S4(b)) at the end of which we can see that the peak in the CV completely disappears, shown as the blue curve in figure S4(a). Due to the large amount of copper here we can also see the second peak, which appears due to the dissolution of copper through the formation of Cu^{2+} ions from Cu^{+} (see figure S4(b)). The e-etching process requires 42 scan cycles in this case in order to completely get rid of the oxidation peak, due to the presence of a thicker (10 nm in comparison to traces in graphene) copper layer here. These results present a definitive confirmation that the traces of copper / copper oxide on graphene are indeed removed using our e-etching procedure.

IV. TOF-SIMS measurements to estimate the relative amount of copper

The presence of copper and its removal after e-etching were also confirmed using time-of-flight secondary ion mass spectrometry (TOF-SIMS). For this purpose three sets of samples were prepared: (1) bare Pt on Si/SiO_2 (2) transferred graphene on Pt on Si/SiO_2 and (3) e-etched graphene on Pt on Si/SiO_2. We chose to use TOF-SIMS in order to have access to a very low detection limit. The amount of copper may be down to the ppm range after graphene transfer as has been shown by inductively coupled plasma – mass spectrometry (ICP-MS) data on transferred CVD-graphene grown on nickel. [17] We chose to use TOF-SIMS in order to avoid any kind of contamination which may creep in during the sample preparation for ICP-MS. Also we did not choose X-ray photoelectron spectroscopy (XPS) in order to obtain an estimate of the amount of copper left after e-etching, which we expected to be very low. Mass spectra were acquired in positive ion mode using a gallium ion source in a commercial TOF-SIMS machine from ION-TOF GmbH (http://www.ion-tof.com/). Secondary ions from an area of 2 mm^2 were collected by the TOF-MS. The intensities of the copper peaks normalized to the platinum peaks are listed in table ST1a. We see that copper is not present on the bare Pt sample (1) serving as a good negative control. On transferred graphene samples we see the presence of copper as exemplified by the large intensities at the m/z values for ^{63}Cu and ^{65}Cu, while on e-etched samples the intensity had reduced to at most 10%

and at best 3% of the initial value, suggesting that more than 90% of the copper was removed using our e-etching procedure. Similar values were obtained by normalizing the peak intensities to the carbon peak as well (table ST1b). Please note that we cannot quantify the amount of copper, due to the large difference in sensitivity of the detector to the various analyzed elements.

Table ST1(a) : Summary of TOF-SIMS results before and after e-etching normalized to the intensity of ^{195}Pt peak. #1 and #2 correspond to two different locations.

Sample	Peak intensities of ^{63}Cu (m/z: 62.9295)		Peak intensities of ^{65}Cu (m/z: 64.9287)	
	Normalized to ^{195}Pt peak	relative amount of copper	Normalized to ^{195}Pt peak	relative amount of copper
(1) bare Pt	0.0004	0.00 %	0.0028	0.00 %
(2) transferred graphene on Pt	2.5862	**100 %**	2.6140	**100 %**
(3) #1. After e-etching	0.1860	7.19 %	0.2027	7.75 %
(3) #2. After e-etching	0.2430	9.39 %	0.2544	9.73 %

Table ST1(b) : Summary of TOF-SIMS results before and after e-etching normalized to the intensity of ^{12}C peak. #1 and #2 correspond to two different locations.

Sample	Peak intensities of ^{63}Cu (m/z: 62.9295)		Peak intensities of ^{65}Cu (m/z: 64.9287)	
	Normalized to ^{12}C peak	relative amount of copper	Normalized to ^{12}C peak	relative amount of copper
(1) bare Pt	0.0213	0.08 %	0.1654	0.64 %
(2) transferred graphene on Pt	25.3762	**100 %**	25.6491	**100 %**
(3) #1. After e-etching	0.8799	3.47 %	0.9589	3.74 %
(3) #2. After e-etching	1.4447	5.69 %	1.5127	5.90 %

In order to arrive at the amount of copper after e-etching, we assume that the intensity of Cu on transferred graphene corresponds to 100% and normalize the other intensities to this peak intensity. It is apparent that we still have some copper left after e-etching. This may be due to

copper trapped between the graphene and the underlying Si/SiO_2 which is most likely not accessible to the e-etching solution.

V.Hall Mobility measurements

In figure 3(c) the increase in maximum mobility is ~60 %. We have observed mobility improvements in the range of 15 – 80 % for the other samples. The mobility improvement is higher for electrons than for holes. The hole mobility increases mainly because of a suppression in charge carrier scattering due to metal impurities, while for electrons there is an additional contribution from the removal of charge transfer due to copper. Moreover we even observe a reduction of charge carrier density around the Dirac point signifying a reduced charge inhomogeneity there (see figure S6). Specifically, we have a reduction in inhomogeneity (calculated using the full-width half maximum of the gate dependence of resistance) from 2 x 10^{12} to 1.4 x 10^{12} cm^{-2}, a factor of around 30%. In other samples this value is in the range of 25 - 89 %. The variation in the improvement is most likely due to a differing density of metal traces from one sample to the other. Although these factors represent modest improvements, they are consistent with the reduction of additional phonon scattering (on top of scattering from SiO_2) that is most likely introduced through the trace metal impurities. All these aspects confirm that the e-etching procedure indeed improves the electronic properties of transferred graphene. Hence, using the e-etching procedure on suspended graphene or on graphene on hBN it can be expected that we might see a considerable improvement in the charge transport properties of CVD-grown graphene, thereby constituting an important and necessary step in order to attain a performance approaching that of exfoliated graphene devices.

V. Supporting References

[30] Bjorndahl, W.D., Nobe, K. *Corrosion* **40**, 82-87 (1984); Russell, R.P., White, A. *Ind. Eng. Chem.* **19**, 116 (1927).

[31] Verink, E.D. *Chapter 6. Simplified procedure for consructing Pourbaix diagrams* in Uhlig's Corrosion Handbook, Second Ed., (Ed.) R.W. Revie, (Wiley: 2000).

[32] Beverskog, B., and Puigdomenech, I. *J. Electrochem. Soc.* **144**, 3476 (1997).

[33] Tromans, D. And Sun, R. *J. Electrochem. Soc.* **11**, 3235 (1991).

[34] Inagaki, M. et al., *Adv. Mater.* **24**, 2547 (2012).

Figure S1. Complete cyclic voltammograms of the curves presented in figure 1 for: A) graphene on Cu foil, B) graphene transferred by etching the copper foil for 15 min. in HCl / H_2O_2 (removal of Cu from below graphene) and C) after additional etching of transferred graphene in a dilute HCl / H_2O_2 solution (removal of Cu also above graphene). The appearance of the reduction peaks in the reverse scan suggests that we are observing the redox process of traces of solid Cu on the graphene surface. Supporting electrolyte: phosphate buffer 0.1 mol L^{-1}, pH 7. Scan rate : 50 mV s^{-1}. T=25°C, in ambient.

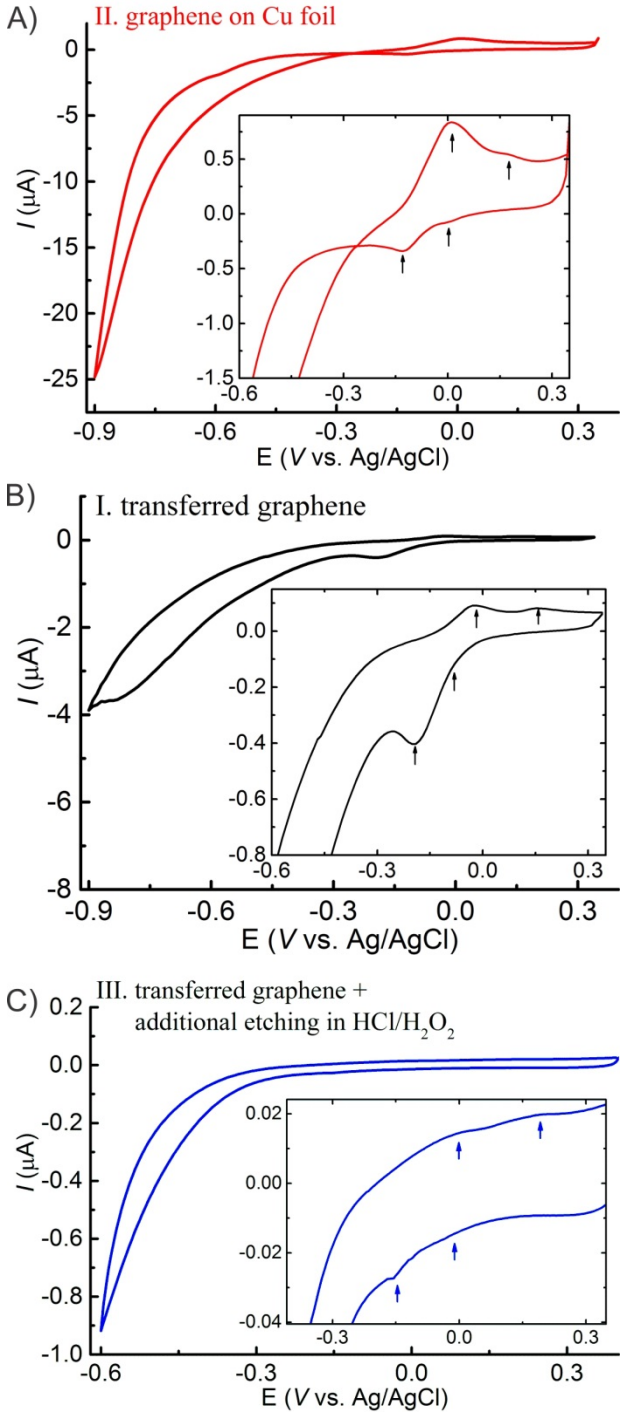

Figure S2. Cyclic voltammograms of the same transferred graphene in two different buffers (phosphate buffers: pH 7 and pH 8, 0.1 mol L^{-1}) showing the oxidation peaks of Cu. It is apparent that the peaks shift to more negative voltages consistent with the Pourbaix diagram in figure 1B. Scan rate : 50 mV s^{-1}. T=25°C, in ambient.

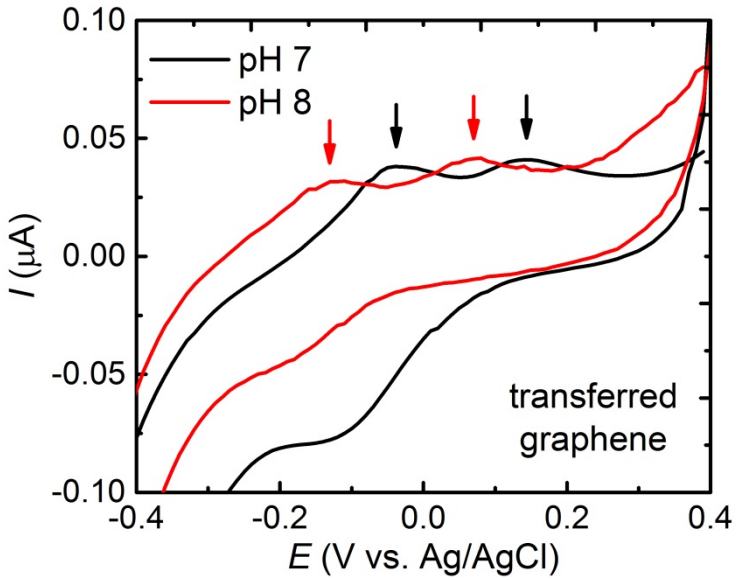

Figure S3a. Complete CVs of the curves shown in figure 2A. The CVs are shown for transferred graphene during e-etching in 0.1 mol L^{-1} HCl. Scan rate : 50 mV s^{-1}. T=25°C, in ambient.

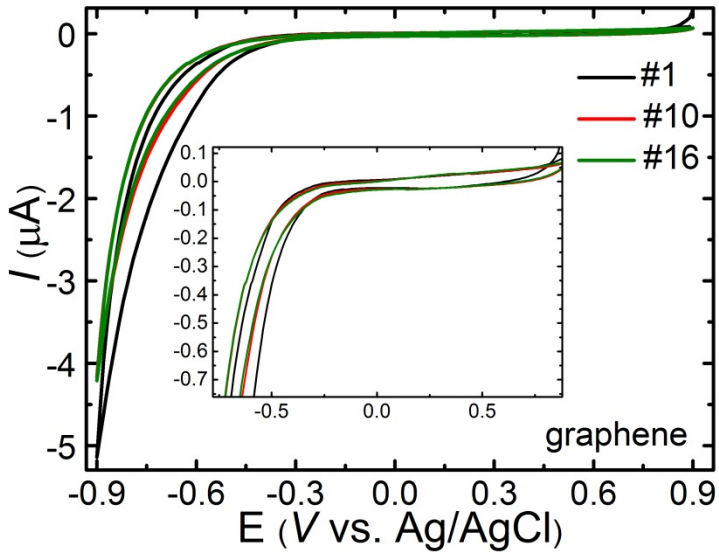

Figure S3b. Another example of e-etching of a transferred graphene sample without removal of copper from the top (no additional dip in HCl/H_2O_2). The baseline-subtracted peak current can be monitored continuously as a function of the CV cycle to directly infer the removal of copper traces. The peak current is extracted from the CVs in the inset measured during e-etching in 0.1 mol L^{-1} HCl. Scan rate : 50 mV s^{-1}. T=25°C, in ambient. In this case the electroactive Cu is completely removed already after 8 cycles.

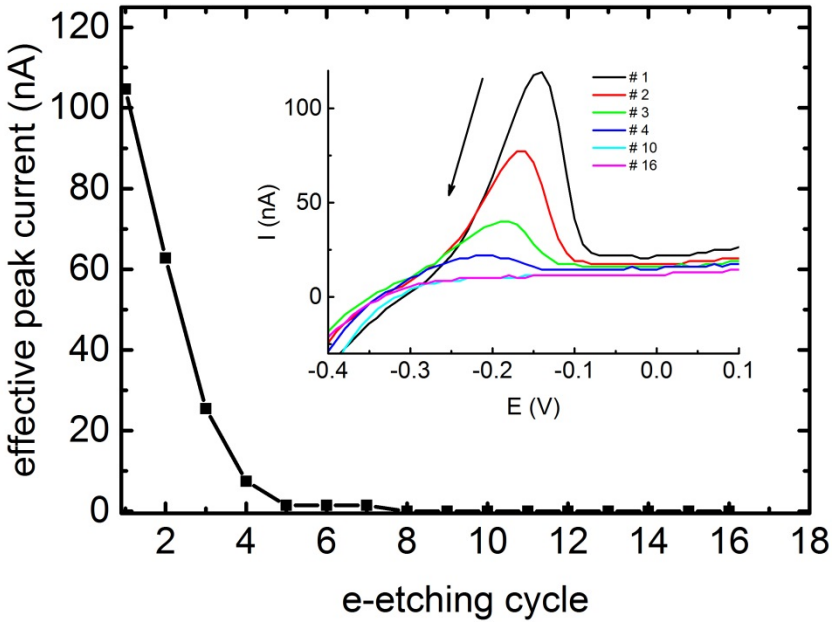

Figure S4. (a) CV in 0.1 mol L^{-1} HCl of pristine flexile carbon fiber (FCF, black curve), FCF with 10 nm of deposited copper (FCF/Cu, red curve) and FCF/Cu after e-etching (blue curve). (b) e-etching of FCF/Cu in 0.1 mol L^{-1} HCl during 42 cycles. Scan rate : 100 mV s^{-1}. T=25°C, in ambient.

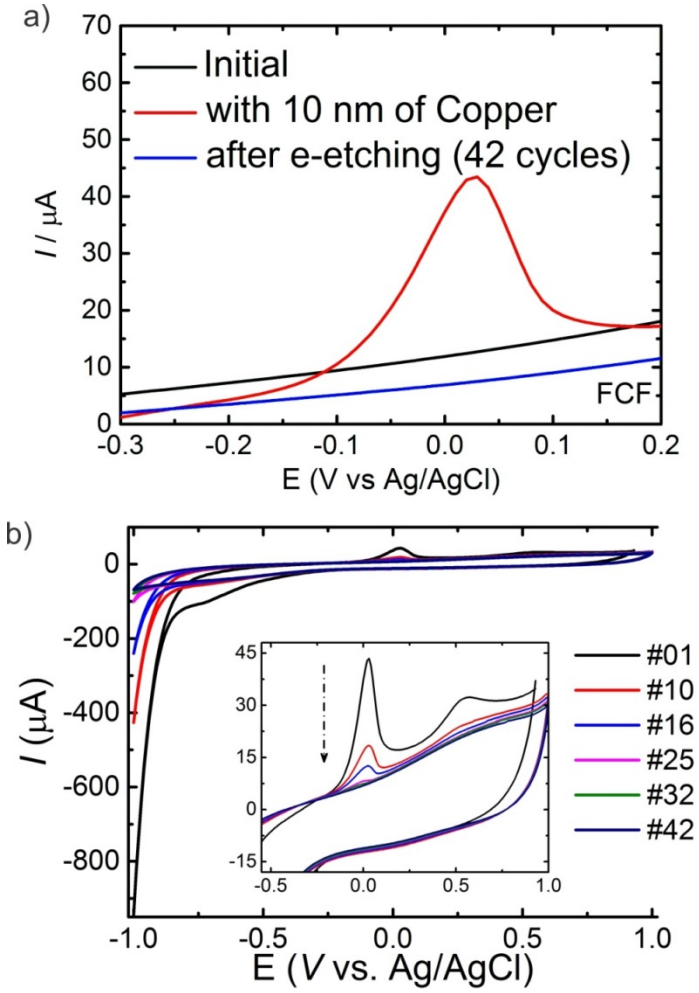

Figure S5. AFM and Raman spectroscopy on the sample of fig.2. (A,B) AFM images obtained at the same position on graphene before (A) and (B) after the e-etching procedure. (C,D) height profiles across the white line in the AFM images before (C) and after (D) e-etching. The scale bar in (A) shows a relative height from -3.9 to 3.5 nm, while in (B) from -4.9 to 5.8 nm. In some areas we see a reduction in particle density, however, not always on all samples. (E) Raman spectrum of graphene after e-etching showing almost zero intensity at the D-peak. Based on the D-to-G-peak intensity ratio (0.04 here), together with the full width half maximum of 2D and G peaks we arrive at the defect density range of 54 to 72 nm. [32] Laser wavelength: 633 nm, 2.7mW, acquisition time : 5s. From (C,D) we can extract an increase in height from 0.5 nm ± 0.2 nm to 1.6 nm ± 0.2 nm. We have seen a similar increase in all the samples investigated. We attribute the cause of this increase to the removal of impurities on the underlying substrate after prolonged exposure to HCl during the e-etching procedure. The *G* and *2D* peaks in (E) confirm that we are indeed observing an area containing monolayer graphene.

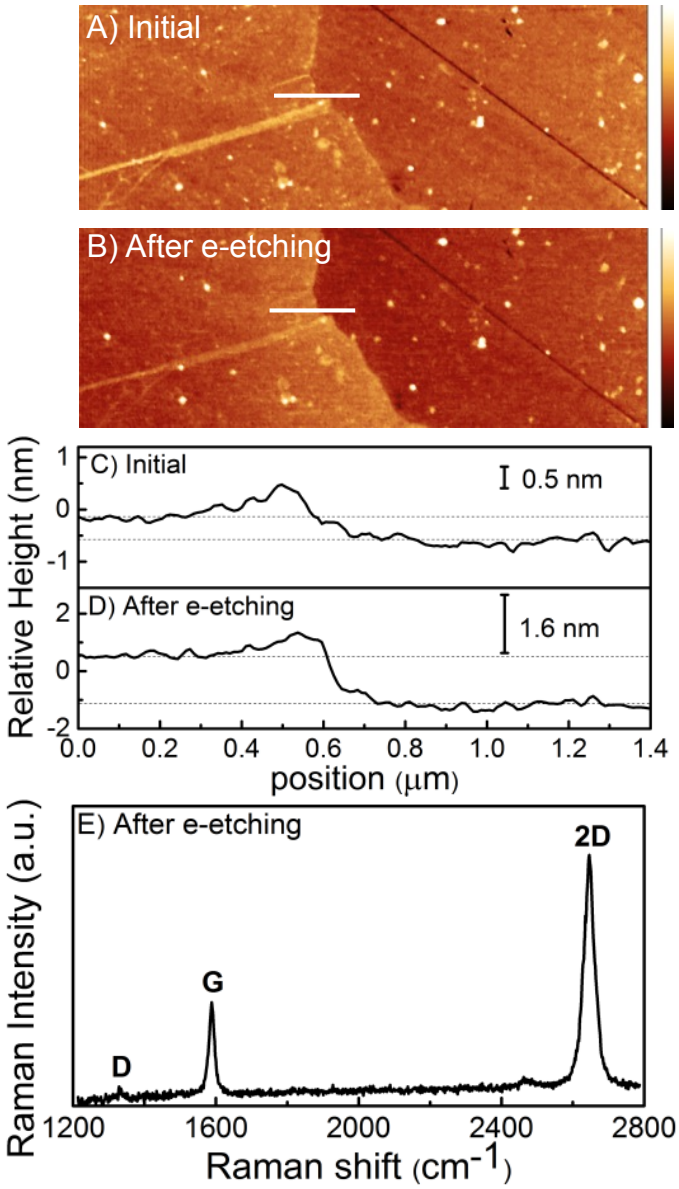

Figure S6. Charge carriers in e-etched graphene. The curves present the same data set as in figure 4 in a different form. (A) Zoom-in view of n vs. V_{IG} showing that the electric field now allows the access to lower carrier densities than before e-etching. (B) Hall mobility as a function of liquid gate voltage and (C) R_{xx} as a function of charge carrier concentration. (pH 7, 0.1 molL^{-1})